J.Serb.Chem.Soc. 66(11–12)935–952(2001) UDC 621.357.7+669.3:541.183+546.33'131
JSCS – 2916 *Original scientific paper*

Copper electrodeposition from a copper acid baths in the presence of PEG and NaCl*

V. D. JOVIĆ#1 and B. M. JOVIĆ2#

Materials Engineering Department, Drexel University, Philadelphia, PA 19104, USA

(Received 7 June 2001)

Copper electrodeposition from copper acid solutions containing PEG and NaCl has been investigated onto Cu(111), Cu(100) and polycrystalline copper electrodes using polarization and EIS measurements. The adsorption of sulphate and chloride anions, and PEG molecules, was investigated onto Cu(111) and Cu(100) by cyclic voltammetry and differential capacitance measurements. Differential capacitance *vs*. potential curves recorded onto Cu(100) in solutions containing 0.1 M H_2SO_4, 0.1 M H_2SO_4 + 10^{-3} M PEG and 0.1 M H_2SO_4 + 10^{-3} M PEG + 10^{-3} M NaCl confirm that "specific adsorption" of PEG molecules occurs in the absence of NaCl in the solution, in the potential region of copper electrodeposition, *e.g.,* between –1.0 V and –0.5 V *vs*. SSE. In the presence of chloride ions, the adsorption of PEG molecules is suppressed and there is no evidence of adsorption of neutral PEG molecules. It is shown that hysteresis, appearing on the polarization curves of copper electrodeposition, is not a consequence of competition between inhibition provided by the Cl-PEG/Cu^{2+}/Cu^{+}/Cu interface and the catalytic effects of Cl-MPSA/Cu^{2+}/Cu^{+}/Cu interaction, because hysteresis is present in the solution containing only PEG and NaCl, *e.g.,* in the absence of MPSA. EIS measurements confirm the simultaneous occurrence of two processes during copper electrodeposition: deposition of copper by discharge of Cu^{2+} ions and "specific adsorption" and discharge of some heavily charged species, most probably containing Cu, PEG and Cl.

Keywords: copper, electrodeposition, PEG, chloride, complexes, Cu(111), Cu(100), adsorption, differential capacitance.

INTRODUCTION

In modern electroplating industry copper is rapidly being introduced into chip interconnection technology as a replacement for aluminum. Current and future feature scaling requires metallization into vias and trenches with aspect ratios as high as 10:1. An advan-

* Dedicated to Professor Dragutin M. Dražić on the occasion of his 70th birthday.

Serbian Chemical Society active member.

1 On leave of absence from the Center for Multidisciplinary Studies University of Belgrade, P.O. Box 33, 11030 Belgrade, Yugoslavia

2 On leave of absence from the Institute of Technical Sciences SASA, P.O. Box 745, 11001 Belgrade, Yugoslavia.

tage of copper electrodeposition over aluminum physical deposition is the ability to "superfill" high aspect ratio feature when plating baths containing additives are usde. Two additives often incorporated into industrial plating baths for such purpose are poly(ethylene glycol) (PEG) and chloride ions, among other additives known as brighteners (molecules with thiol and sulphonic acid groups) and levelers (typically molecules having amine functionality).[1–9] Although a phenomenological understanding of the influence of these additives exists their mode of action on a molecular level is lacking.

A number of studies of the mechanism of copper electrodeposition in the absence of additives have confirmed that deposition occurs in a two-step process with cupric-to cuprous ion reduction being the rate determining step af high current densities.[10–14] The addition of a small amount of chloride ions (2×10^{-4} M) was found to modify the electrode kinetics essentially by increasing the transfer coefficient of the reaction of cuprous ion reduction.[15] If both PEG and chloride ions are present in the acidic copper sulphate bath, the significant inhibition of copper electrodeposition has been explained by various authors. Hill *et al.*[16] found that below the critical overpotential, chloride ions hold a film of PEG onto the electrode surface and that this film may be a PEG-cuprous chloride complex. Healy *et al.*[17] suggested that PEG can be adsorbed in two different forms. One predominates close to the open circuit potential and may well be a copper chloride complex with PEG as a ligand, while the other one prevails at the more negative potentials where copper plating is performed and this species is likely to be a simple, neutral PEG molecule. According to the hypothesis of Yokoi *et al.*[18,19] each Cu^+ ion present in an acidic copper bath orientates six electron pair donor oxygen atoms of poly(ethylene oxide) chains forming a positively charged complex of the type $\{Cu+(EO)_6\}$. As a result of their positive charge, these are attracted by the negatively charged chloride ions specifically adsorbed onto the copper surface, inhibiting copper electrodeposition. At a difinite potential, the Cu^+-oxygen atoms bonds break and liberate Cu^+ ions whereby copper deposition suddenly commences, while PEG returns to the bulk electrolyte. Stoychev *et al.*[20] studied the interaction of PEG with Cu^+ and Cu^{2+} ions in aqueous acidic media by specific electrical conductivity, optical density and cyclic volatmmetry measurements. They found that in the absence of chloride ions complexes of the types $\{Cu^+(–EO–)_3(x–1)H_2O\}$ and $\{Cu^{2+}(–EO–)_4(y–1)H_2O\}$ can be formed. In the case when $\{–CH_2CH_2–O–\}_n$ and $Cl^–$ are both present in the acid copper electrolyte, the simultaneous formation of complexes between both copper ions and ethylene oxide units and copper ions and chloride ions is possible. Three types of these complexes could be formed: $H^+\{–EO–\}_nCl^–$; $H^+\{–EO–\}_nCuCl_3^–$ and $H^+\{–EO–\}_nCuCl_2^–$. Stoychev *et al.*[21,22] also studied the adsorption of PEG onto polycrystalline[21] and monocrystalline[22] copper surfaces in KF solution by differential capacitance measurements. According to their results, very weak adsorption of PEG was detected in the potential region of copper electrodeposition (300 mV to 100 mV *vs*. NHE). Recently, Kelly *et al.*[23,24] performed a quartz crystal microbalance study and found that the inhibition of copper deposition is the consequence of the adsorption of a monolayer of PEG molecules that are collapsed into spheres provided chloride ions are present, while little adsorption of PEG can occur in the absence of chloride ions. They also developed a model that only assumes the adsorption of nearly a

monolayer of PEG in the presence of chloride ions, as well as the adsorption of Cu^+ species (Cu^+_{ads}) which was sufficient to explain the steady-state and EIS measurements on a rotating disc electrode, *i.e.* in the case of convective diffusion.

In the present work, the polarization characteristics of copper deposition onto polycrystalline and monocrystalline, Cu(111) and Cu(100), copper electrodes were investigated in the presence of three different PEG concentrations (10^{-5} M, 10^{-4} M and 10^{-3} M), each of them in the absence and in the presence of chloride ions (10^{-6} M, 10^{-5} M, 10^{-4} M and 10^{-3} M). EIS measurements at a constant current and a constant potential were performed in all solutions on polycrystalline copper electrode. Cyclic voltammetry and differential capacitance measurements were used for the investigation of adsorption of sulphate ions, PEG molecules and chloride ions onto Cu(111) and Cu(100) faces.

EXPERIMENTAL

All experiments were carried out in a two-compartment electrochemical cell at 25 ± 1 ºC in an atmosphere of purified nitrogen. The polycrystalline and monocrystalline electrodes (d = 2.54 cm) were sealed in epoxy resin (resin EPON 828 + hardener TETA) in such a way that only the (111), or (100), or polycrystalline disc surface was exposed to the solution. The surface area of the electrode exposed to the electrolyte was 5.05 cm^2. The counter electrode was a platinum sheet which was placed parallel to the working electrode. The reference electrode was a saturated sulphate electrode (SSE), which was placed in a separate compartment and connected to the working compartment by means of a Luggin capillary. All solutions were made from supra pure (99.999 %) chemicals (Aldrich) and EASY pure UV water (Barnstead).

The copper single and poly crystals (Monocrystals Comp.) were mechanically polished on fine grade emery papers (1200, 2400 and 4000) with subsequent polishing on polishing clothes impregnated with a suspension of polishing alumina with particles dimension of 1 μm, 0.3 μm and 0.05 μm. After chemical polishing all electrodes were electrochemically polished in a solution of 85 % phosphoric acid at a constant voltage of 1.7 V (*vs*. Pt counter electrode) until the current density dropped to a value of about 18 mA cm^{-2}. The electrodes were then thoroughly washed with pure water (Barnstead - EASY pure UV) and transferred to the electrochemical cell.

Cyclic volatammetry and polarization experiments were performed using a universal programmer PAR M-175, a potentiostat PAR M-173 and *X*–*Y* recorder (Houston Instrument 2000R). A universal programmer and a potentiostat in conjuction with a computer were also used for recording polarization diagrams (recorded at a sweep rate of 1 mV s^{-1}) and cyclic voltammograms. EIS measurements were performed using a potentiostat PAR M-273A and an impedance/gain-phase analyzer (Schlumberger SI 1260) in conjunction with a PC computer. The Z-plot programme (version 2.3) was used for performing the experiments and fitting the experimentally obtained results. Differential capacitance *vs*. potential dependence was obtained from impedance measurement at low frequencies (see Results).

RESULTS

Polarization diagrams of copper electrodeposition

Polarization diagrams of copper electrodeposition on the electrochemically polished polycrystalline copper electrode were recorded (at the sweep rate of 1 mV s^{-1}) in solutions containing 0.25 M $CuSO_4$ + 1.8 M H_2SO_4 + x M PEG, with x being 10^{-5} M, 10^{-4} M and 10^{-3} M. In each of these solutions, the concentration of Na Cl was varied from 0 M to 10^{-3} M (0 M, 10^{-6} M, 10^{-5} M, 10^{-4} M, and 10^{-3} M). Each diagram was recorded starting from the open circuit potential (usually about – 0.4 V *vs*. SSE) and changing the potential towards

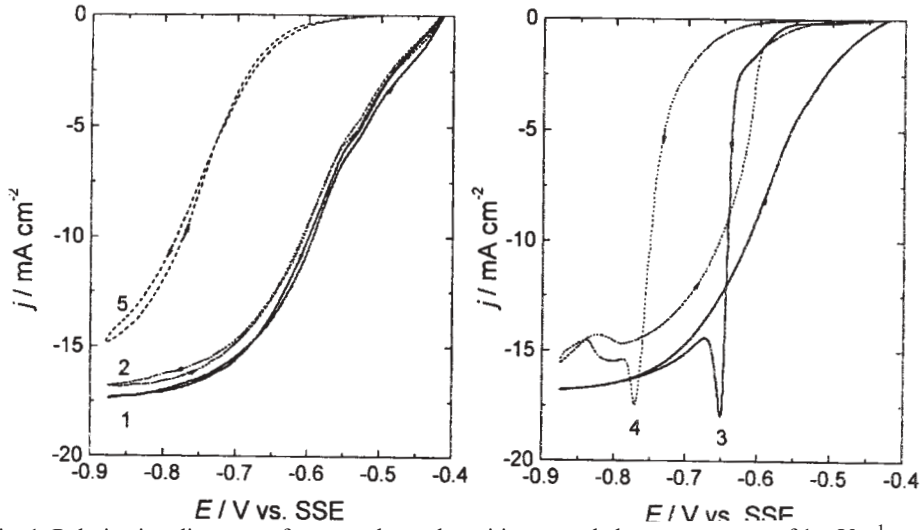

Fig. 1. Polarization diagrams of copper electrodeposition recorded at a sweep rate of 1 mV s^{-1} onto a polycrystalline copper electrode in solutions containing 0.25 M $CuSO_4$ + 1.8 M H_2SO_4 + 10^{-3} M PEG + x M NaCl: (1) $x = 0$; (2) $x = 10^{-6}$ M; (3) $x = 10^{-5}$ M; (4) $x = 10^{-4}$ M; (5) $x = 10^{-3}$ M.

more negative vaues up to about –0.9 V *vs*. SSE and back to the open cicruit potential. It was found that the concentration of PEG has practically no influence on the shape of the polarization diagrams, while the concentration of chloride ions significantly influence the shape and position of the polarization diagrams.

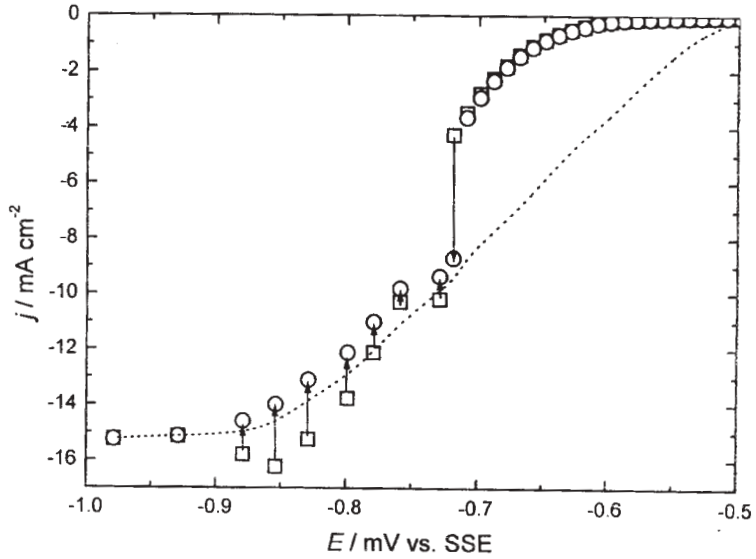

Fig. 2. Stationary potentiostatic curve for copper electrodeposition recorded onto polycrystalline copper electrode in a solution containing 0.25 M $CuSO_4$ + 1.8 M H_2SO_4 + 10^{-3} M PEG + 10^{-4} M NaCl.

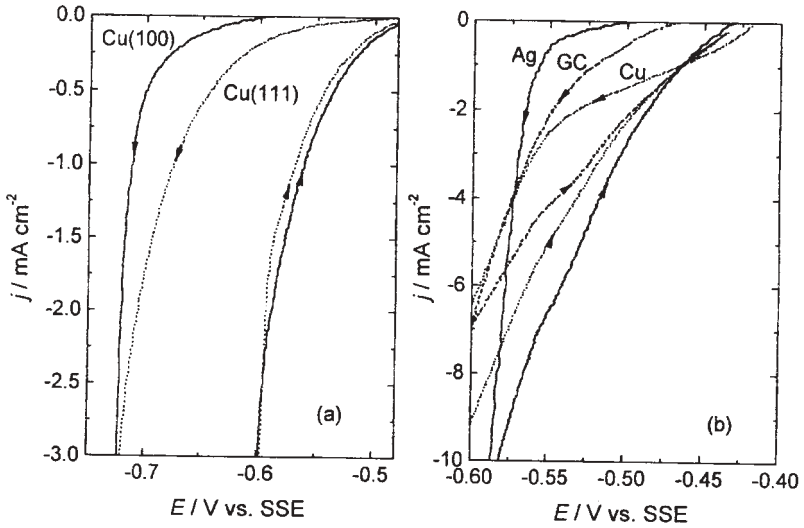

Fig. 3. Polarization diagrams of copper electrodeposition recorded at a sweep rate of 1 mV s^{-1} onto Cu(111), Cu(100), polycrystalline copper (Cu), polycrystalline silver (Ag) and glassy carbon (GC) electrodes in a solution containing 0.25 M $CuSO_4$ + 1.8 M H_2SO_4 + 10^{-3} M PEG + 10^{-5} M NaCl.

Typical results are shown in Fig. 1 for 10^{-3} M PEG. As can be seen, increasing the chloride ions concentration inhibits the process of copper deposition (diagrams 2–5). It is interesting to note that almost identical polarization diagrams were obtained in both directions for the solution free of chloride ions (1), the solution with the lowest Cl^- concentration (2) and the solution with the highest Cl^- concentration (5). For the two intermediate Cl^- concentrations (3 and 4), pronounced hysteresis was obtained.

Since the hysteresis could be a consequence of the applied sweep rate of 1 mV s^{-1}, a stationary potentiostatic diagram, shown in Fig. 2, was recorded in the solution containing 10^{-3} M PEG + 10^{-4} M NaCl (a solution typical for the appearance of hysteresis). The potential was changed in steps of 10 mV and 20 mV from the open circuit potential towards more negative values. The current densities were recorded immediately after applying a certain potential (squares) and after about 10 min when a stable current density had been established (circles). As can be seen, a very small increase in the current density with time was recorded in the potential region from –0.50 V to –0.71 V *vs.* SSE. At a potential of –0.72 V *vs.* SSE, the significant increase in the current density indicates the commencement of massive copper deposition (the direction of the change of the current density is marked with the arrows). At potentials between –0.72 V and –0.88 V *vs.* SSE, a decrease of the current density with time was recorded, while at potentials more negative than –0.88 V *vs.* SSE, identical values of the current densities were recorded immediately after the application of the potential and after 10 min. When going back to the open circuit potential, the current densities were stable at all potentials applied (they did not change with time) and this curve is presented with dotted line. From the chape of this diagram it can be concluded that the hysteresis is not a consequence of the sweep rate used for recording polarization diagrams.

Polarization diagrams of copper deposition from the solution containing 10^{-3} M PEG + 10^{-4} NaCl (typical for the appearance of hysteresis) were recorded on Cu(111) and Cu(100) faces. As can be seen in Fig. 3a, the copper deposition commences at more negative potentials onto Cu(100) than onto Cu(111), while polarization diagrams obtained by going back to more positive potentials are identical. Hysteresis is also present on both single crystal faces.

Polarization diagrams of copper deposition from the solution containing 10^{-3} M PEG + 10^{-5} M NaCl (also typical for the appearance of hysteresis) were recorded on three different substrates, electrochemically polished polycrystalline Ag and Cu electrodes, and on a mechanically polished glassy carbon (GC) electrode. As can be seen in Fig. 3b, copper deposition is more inhibited on GC and Ag electrodes than on the Cu electrode, with hysteresis being present on all three substrates. It should be mentioned here that these experiments were also performed on Ag, Cu and GC electrodes rotating at 1000 rpm., and that in all cases hysteresis was detected.

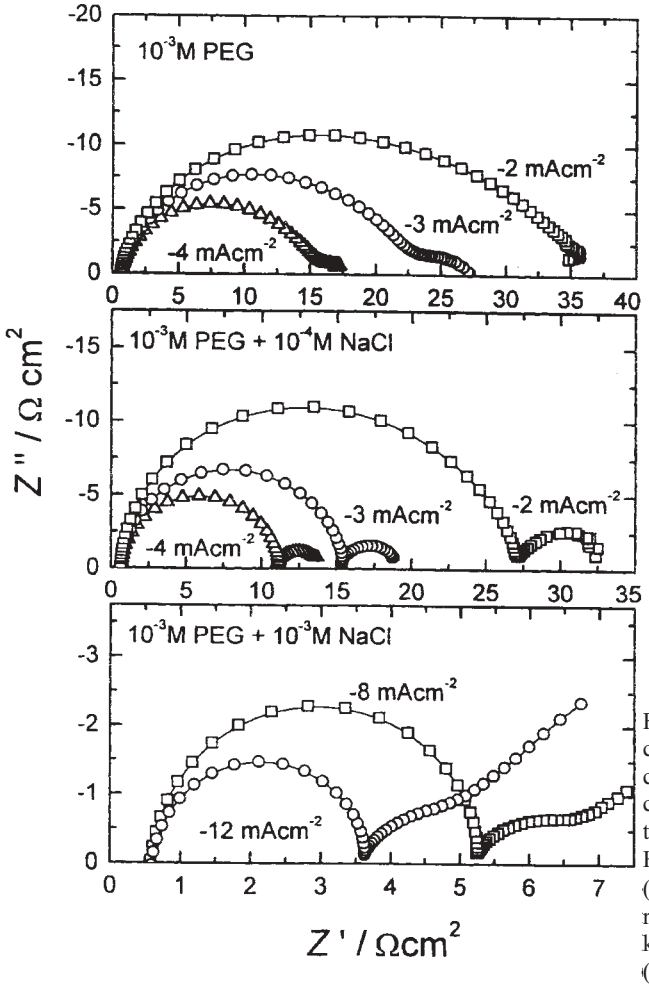

Fig. 4. Typical Z'–Z'' diagrams of copper electrodeposition recorded onto a polycrystalline copper electrode in solutions containing 0.25 M $CuSO_4$ + 1.8 M H_2SO_4 + 10^{-3} M PEG + x M NaCl ($0 \leq x \leq 10^{-3}$) in the frequency range between 0.05 Hz and 30 kHz at different current densities (marked in the Figure).

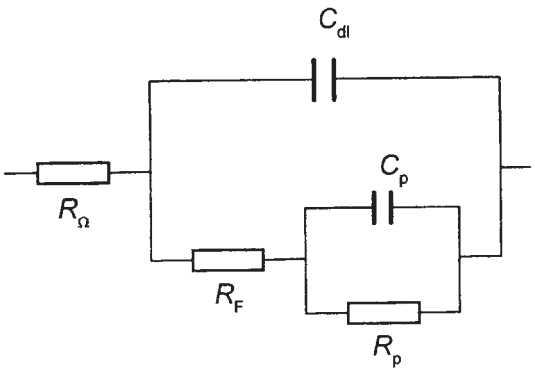

Fig. 5. Equivalent circuit used for fitting the experimentally recorded Z'–Z'' diagrams: R_Ω – ohmic resistance between the Luggin capillary and working electrode surface; C_{dl} – double layer capacitance; R_F – Faradaic resistance (deposition of copper by discharge of Cu^{2+} ions); C_p – pseudo-capacitance (specific adsorption of species containing Cu, PEG and Cl); R_p – charge transfer resistance corresponding to the discharge of specifically adsorbed species.

EIS measurements

Typical results of EIS measurements, recorded on a polycrystalline copper electrode in the frequency range from 0.05 Hz to 30 kHz in a solution containing 10^{-3} M PEG (very similar results were obtained with the other two PEG concentrations), are shown in Fig. 4. Almost identical Z'–Z" diagrams, recorded in the region of activation controlled deposition (up to a current density of 5 mA cm^{-2}) were obtained in the solutions containing 10^{-3} M PEG, 10^{-3} M PEG + 10^{-6} M NaCl and 10^{-3} M PEG + 10^{-5} M NaCl (the diagram recorded in 10^{-3} M PEG solution is presented). As can be seen, indications of the presence of a second semi-circle can be recognized at current densities of 2 mA cm^{-2} and 3 mA cm^{-2}. Two very well defined semi-circles were obtained in the so-

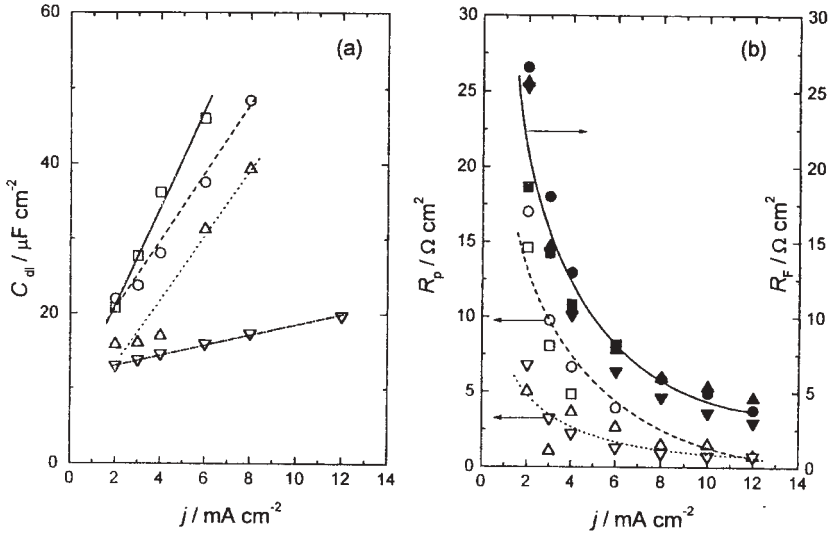

Fig. 6. (a) C_{dl} as a function of current density during the electrodeposition of copper from a solution of 0.25 M $CuSO_4$ + 1.8 M H_2SO_4 + 10^{-3} M PEG containing different concentrations of NaCl; (b) R_F and R_p as a function of current density during the electrodeposition of copper from a solution of 0.25 M $CuSO_4$ + 1.8 M H_2SO_4 + 10^{-3} M PEG containing different concentrations of NaCl. (□■) 10^{-6} M NaCl; (○●) 10^{-5} M NaCl; (Δ▲) 10^{-4} M NaCl; (▽▼) 10^{-3} M NaCl.

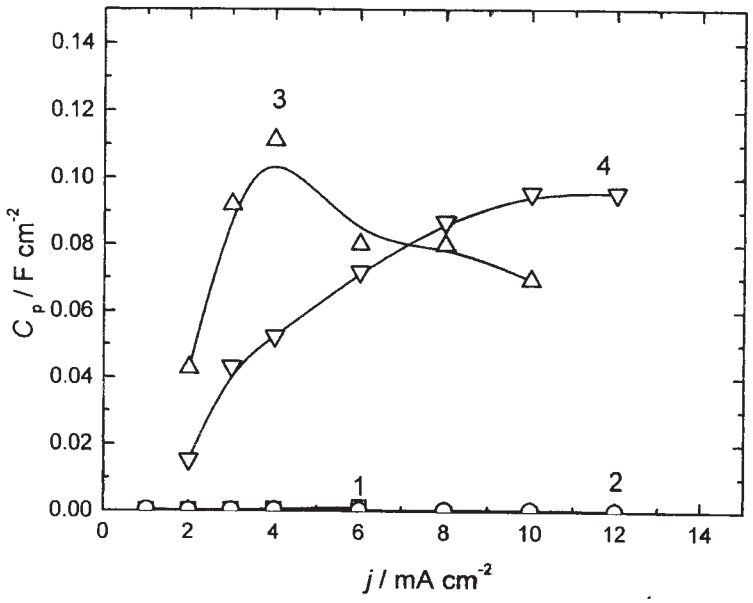

Fig. 7. C_p as a function of current density during the electrodeposition of copper from a solution of 0.25 M $CuSO_4$ + 1.8 M H_2SO_4 + 10^{-3} M PEG containing different concentrations of NaCl: (1 – □) 10^{-6} M NaCl; (2 – ○) 10^{-5} M NaCl: (3 – Δ) 10^{-4} M NaCl; (4 – ▽) 10^{-3} M NaCl.

lutions containing 10^{-4} M NaCl and 10^{-3} M NaCl. An example is shown in Fig. 4 for the solution containing 10^{-3} M PEG + 10^{-4} M NaCl. The presence of Warburg impedance at higher current densities indicates the influence of diffusion, since the current values approach the diffusion limiting current density for copper deposition. An example is shown for the solution containing 10^{-3} M PEG + 10^{-3} M NaCl.

The experimentally recorded results were fit with the equivalent circuit presented in Fig. 5. Very good fits were obtained for all the EIS results.

The double layer capacitance (C_{dl}) values varied between 15 μF cm^{-2} and 40 μF cm^{-2}, increasing linearly with increasing current density for all the investigated solutions, as shown in Fig. 6a. The values of R_F and R_p were found to depend exponentially on the current density for all solutions, as shown in Fig. 6b, with R_F being practically indepentendt of the PEG and NaCl concentrations, while the values of R_p decreased with increasing NaCl concentration.

The value of pseudo-capacitance, C_p, was found to depend strongly on the chloride ion concentration. As can be seen in Fig. 7a, significant increase in C_p was detected in the solutions containing 10^{-4} M and 10^{-3} M NaCl. Extremely high values for C_p, varying from 0.02 F cm^{-2} to 0.11 F cm^{-2}, obtained at higher concentrations of chloride ions indicate very strong adsorption of some heavily charged species. At lower NaCl concentrations (10^{-5} M and 10^{-6} M), as well as in the solution containing only PEG molecules, the values of C_p were found to increase from about 200 μF cm^{-2} to about 800 μF cm^{-2} with current density.

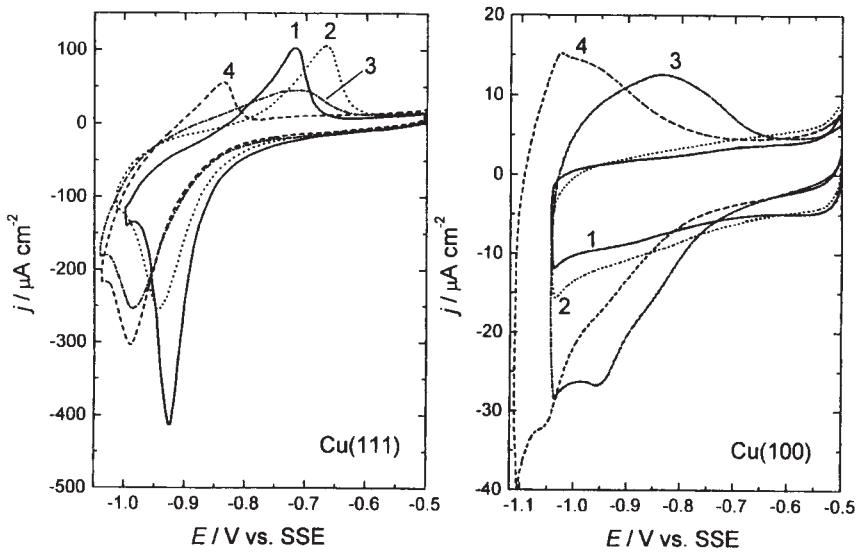

Fig. 8. Cyclic voltammograms recorded onto Cu(111) and Cu(100) at a sweep rate of 100 mV s^{-1} in different solutions: (1) 0.1 M H_2SO_4; (2) 0.1 M H_2SO_4 + 10^{-3} M PEG; (3) 0.1 M H_2SO_4 + 10^{-3} M PEG + 10^{-4} M NaCl and (4) 0.1 M H_2SO_4 + 10^{-3} M PEG + 10^{-3} M NaCl.

Cyclic voltammetry and differential capacitance measurements onto Cu(111) and Cu(100) faces

In order to understand the influence of PEG molecules and anions present in the acid copper solution an the electrodeposition of cupper, cyclic volatammetry and differential capacitance measurements were performed onto Cu(111) and Cu(100) faces in the solutions containing only 0.1 M H_2SO_4 (1), 0.1 M H_2SO_4 + 10^{-3} M PEG (2), 0.1 M H_2SO_4 + 10^{-3} M PEG + 10^{-4} NaCl (3) and 0.1 H_2SO_4 + 10^{-3} M PEG + 10^{-3} M NaCl (4).

The cyclic voltammograms recorded in these solutions onto Cu(111) and Cu(100) at the sweep rate of 100 mV s^{-1} are shown in Fig. 8. As can be seen, two peaks are present in all solutions onto Cu(111) with the peak potentials depending on the composition of the solution. No adsorption peaks can be seen onto Cu(100) in solutions (1) and (2), while in the presence of chloride ions well defined anodic and cathodic peaks indicate adsorption and desorption of chloride ions, respectively, which occur in the potential region between – 0.8 V and – 1.1 V *vs*. SSE.

Differential capacitance values were obtained from impedance measurements at constant potential in the low frequency (from 1 Hz to 100 Hz) region. The differential capacitance is by definition the imaginary component of the electrode admittance over frequency, $C_{diff} = Y''/\omega$. Since the value of C_{diff} could be influenced by the ohmic resistance,[25–27] the imaginary component of the electrode admittance was corrected for ohmic resistance (R_Ω – determined from the highe frequency intercept of the impedance diagrams) by subtracting it from the real component of the electrode impedance, $Z'_{corr} = Z' - R_\Omega$ and calculating Y''_{corr} using the following equation:

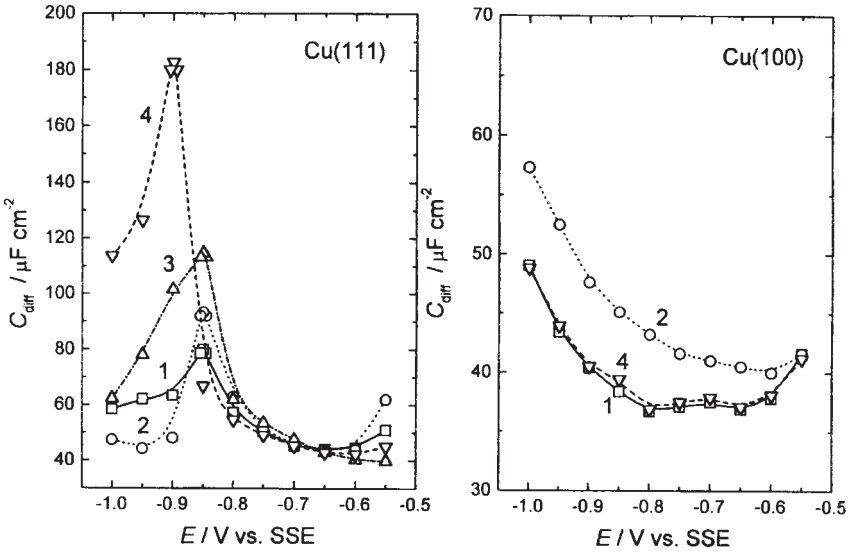

Fig. 9. Differential capacitance *vs*. potential curves recorded onto Cu(111) and Cu(100) in different solutions: (1) 0.1 M H_2SO_4; (2) 0.1 M H_2SO_4 + 10^{-3} M PEG; (3) 0.1 M H_2SO_4 + 10^{-3} M PEG + 10^{-4} M NaCl and (4) 0.1 M H_2SO_4 + 10^{-3} M PEG + 10^{-3} M NaCl.

$$Y''_{corr} = \frac{Z''}{(Z'_{corr})^2 + (Z'')^2} \tag{1}$$

If there is no "specific adsorption", the value of the differential capacitance should be independent of frequency, while in the presence of "specific adsorption", the differential capacitance was found to be dependent on the applied frequency.[25–27] The best way to obtain the "real" value of the differential capacitance is to extrapolate this dependence to zero frequency.[26,27]

In our experiments, these dependences were mainly exponential at frequencies lower than 10 Hz. Linear extrapolation of this part of the dependence was used to extrapolate C_{diff} to zero frequency.

Differential capacitance (corrected for R_Ω) *vs.* potential curves for Cu(111) and Cu(100), recorded in all four solutions, are shown in Fig. 9. As can be seen a maximum on the $C_{diff} - E$ curve recorded using Cu(111) in the pure sulphate solution appears at a potential of about –0.85 V *vs*. SSE (curve 1). This maximum becomes more pronounced on addition of 10^{-3} M PEG (curve 2). In the presence of chloride ions (curves 3 and 4), this maximum increases significantly appearing at a more negative potential with the higher chloride ions concentration (curve 4). Using the (100) face of copper, no maximum was observed in either of these solutions. A small increase of C_{diff} was detected in the potential region from –0.85 V to –1.0 V *vs*. SSE. It is interesting to note that C_{diff} increases on addition of PEG to the sulphuric acid solution (curve 2), while in the presence of chloride ions, the $C_{diff} - E$ curve (curve 4) is indentical to the curve recorded in pure sulphuric acid solution (curve 1).

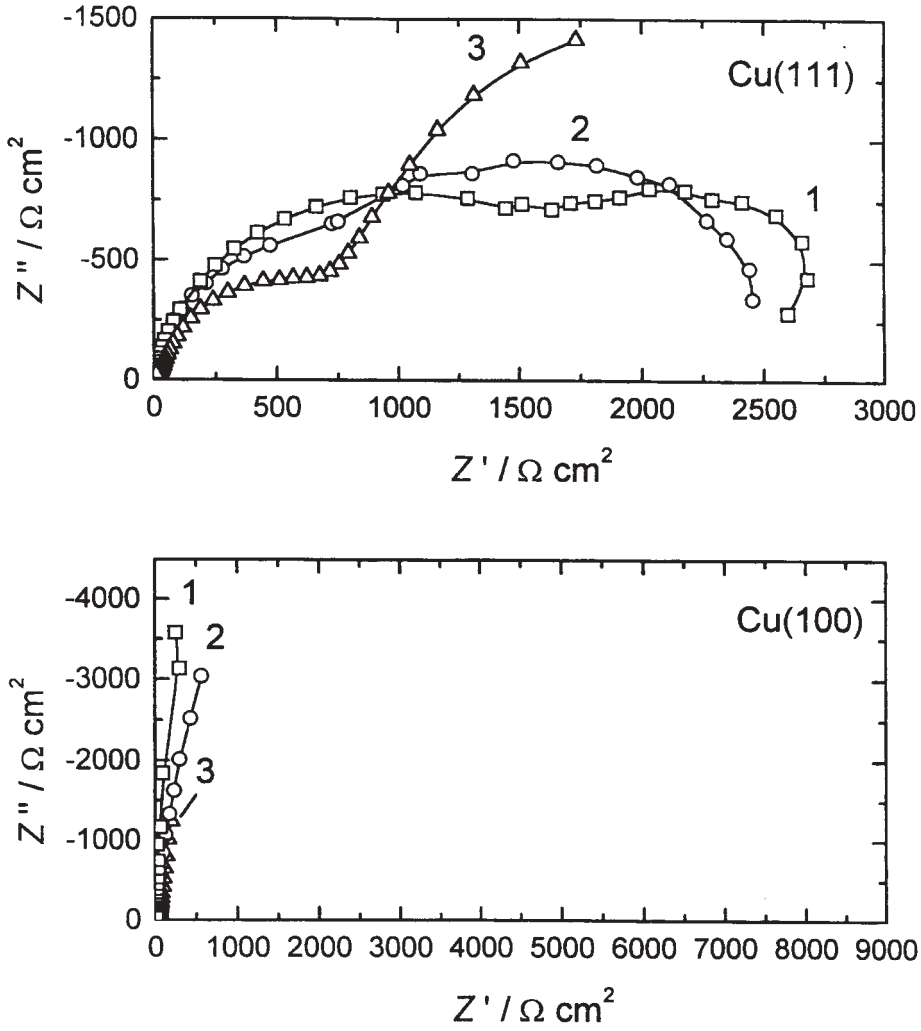

Fig. 10. *Z'–Z''* diagrams recorded onto Cu(111) and Cu(100) electrodes in the frequency ragne between 0.05 Hz and 30 kHz at a potential of – 0.95 V *vs*. SSE in different solutions: (1) 0.1 M H_2SO_4; (2) 0.1 M H_2SO_4 + 10^{-3} M PEG and (3) 0.1 M H_2SO_4 + 10^{-3} M PEG + 10^{-3} M NaCl.

The results of EIS experiments performed in the region of potential where C_{diff} increases on Cu(100) and at the potential of the maximum of the $C_{diff} - E$ curve for Cu(111) in the frequency range between 0.05 Hz and 30 kHz are shown in Fig. 10. As can be seen in the case of the (111) face, the impedance diagrams indicate that two processes are taking place in all solutions at the potential of the maximum of the $C_{diff} - E$ curve, ($E = -0.95$ V *vs.* SSE) while in the case of the (100) face, typical "double layer" impedance diagrams were recorded.

DISCUSSION

Adsorption of PEG onto Cu(111) and Cu(100) faces in the presence of sulphate and chloride anions

Most of the models explaining the influence of PEG on the electrodeposition of copper assume the adsorption of a monolayer of neutral PEG molecules onto the copper surface, as well as the adsorption of different complexes formed between copper ions and PEG molecules.[16–24] Hence, it is important to understand the process of PEG adsorption onto copper monocrystals.

If PEG molecules adsorbs as neutral molecues, the differential capacitance should decrease, since PEG covers part of the surface available for "double layer formation".[28] Considering the resuluts presented in Fig. 9, it is clear that this is not the case. On both faces of copper, the addition of PEG to the sulphuric acid solution does not provoke a decrease but, on the contrary, a small increase of the differential capacitance (curves 2).

In the case of Cu(111) it is found by *in situ* STM measurements that sulphate anions adsorb forming a Moiré pattern,[29] which is suggested to be the consequence of a mismatch of the structure that consists of a $(\sqrt{3} \times \sqrt{7})SO_4^{2-}$ with the (111) structure of a second Cu layer.[30] This structure was found to be stable at potentials more positive than – 0.6 V *vs.* SSE, with a well defined peak of its adsorption between – 0.6 V and – 0.5 V *vs.* SSE. The cathodic peak of the desorption of this structure appeared at a potential of – 0.9 V *vs.* SSE, indicating an irreversible adsorption/desorption process.[29,30] The charge under the cathodic peak was much higher than that needed for the desorption of adsorbed sulphate anions structure and it was supposed that hydrogen evolution occurs during the desorption of sulphate anions.[29,30] It is important to note that the same amount of charge was not obtained for the anodic and cathodic peaks even after subtraction of the hydrogen evolution current from the current of the cathodic peak.[29] Hence, at potentials more negative than –0.8 V *vs.* SSE, simultaneous evolution of hydrogen and desorption of sulphate anios take place on the (111) face of copper. In such a case of an irreversible adsorption/desorption mechanism, the question arises what should be the shape of the $C_{diff} - E$ curve? In our expeirments the same cyclic voltammogram was obtaiine as in the paper of Wilms *et al.*[29,30] (Ref. 29, Fig. 1) after cycling the electrode for 30 min between –1.0 V and –0.5 V *vs.* SSE. After performing impedance measurements at ten potentials with a step of 50 mV (to obtain the $C_{diff} - E$ curve), the cyclic voltammogram changed in such a way that the anodic and cathodic peaks became closer to each other, *i.e.,* less irreversible (Fig. 8, curve 1). According to the impedance diagram (diagram 1) presented in Fig. 10, it is obvious that two processes occur in the potential region of the cathodic peak. After fitting the experimentally recorded *Z'–Z''* diagram with the equivalent circuit presented in Fig. 5, values of C_p of 1000 μF cm^{-2} and C_{dl} of 70 μF cm^{-2} were obtained. Comparing the values of C_{dl} and C_{diff} at this potential, it can be concluded that they are very close (60 and 70 μF cm^{-2}), indicating that the $C_{diff} - E$ curve is not influenced by the simultaneous occurrence of hydrogen evolution. Unfortunately, this was not the case in the presence of PEG and PEG + NaCl, where the obtained C_{dl} values were different to the corresponding C_{diff} values. Hence, it seemed unreasonable to consider the $C_{diff} - E$ curve for the (111) face of copper in order to obtain data about the adsorption of species present in the solution.

On the other hand, the shape of the *Z'–Z''* diagram for Cu(100) at the same potential in all three solutions (Fig. 10) clearly indicate "double layer" properties.[31] Accordingly, the $C_{diff} - E$ curve for the (100) face of copper can be cosidered without any doubt relevant for the adsorption behaviour of species present in the solution. Cosidering Fig. 9, it is obvious that the adsorption of PEG occurs in the potential region of copper deposition on the (100) face of copper. This adsorption has the character of "specific" adsorption (with charge transfer involved) and cannot be treated as adsorption of a neutral molecule, which is in accordance with the results presented by Stoychev *et al.*[21,22] Such behaviour is most probably due to the one hydrogen bonding site, –O–, in the monomer unit of PEG.[20, 32] The presence of the electron-rich oxygen atoms in the backbone structure of PEG offers sites for adsoprtion, as well as for coordination. The "double layer" character of the voltammograms recorded with the (100) face of copper in the presence of sulphate anions (voltammogram 1) and sulphate anions and PEG molecules (voltammogram 2) changes on addition of chloride ions showing well defined and reversible peaks of chloride ions adospriton and desorption in the potential region between – 1.1 V and – 0.8 V *vs*. SSE (Fig. 8, voltammograms 3 and 4). On the other hand, in the presence of chloride anions, the differential capacitance decreases (curve 4, Fig. 9) in comparison with that recorded for sulphate and PEG solution (curve 2), becoming identical to the one recorded in pure sulphuric acid solution (curve 1). According to the findings of Ehlers *et al.,*[33] chloride anions adsorb onto Cu(100) in pure chloride solution forming a $(\sqrt{2} \times \sqrt{2})$R45º structure which is stable up to about – 1.0 V *vs*. SSE. In the presence of sulphate anions, the adsorbed chloride anions are reduced to Cl^- at more positive potentials in comparison with pure chloride solution (at about , – 0.75 V *vs*. SSE), being replaced by sulphate anions adsorbed in the form of a (2 × 2) structure. Since there are no data about sulphate anions adsorption onto Cu(100) in pure sulphate solution, it seems that this structure could be expected in pure sulphate solution, but no speculations about the corresponding $C_{diff} - E$ curve (curve 1) can be made. With addition of 10^{-3} M PEG, weak adsorption of PEG can be seen on the $C_{diff} - E$ curve (curve 2). The amount of PEG adsorbed does not change with potential following the chape of $C_{diff} - E$ curve for pure sulphuric acid solution (curve 1). Such a behaviour could be expected since the (2 × 2) structure of the sulphate anions is an open structure, which allows adsorption of PEG molecules. When chloride anions are added to the solution they form a stable, close packed and discharged $(\sqrt{2} \times \sqrt{2})$R45º structure in the potential region between – 0.8 V and – 0.6 V *vs.* SSE, which prevents the adsorption of PEG molecules. At potentials more negative than – 0.8 V *vs.* SSE, according to Ehlers *et al.,*[33] adsorption of SO_4^{2-} and the simultaneous desorption of Cl^- occur. It is not clear why this process is characterized by an increase in values of the differential capacitance to the same extent as in pure suphuric acid solution (curve 1), but it is obvious that the "specific" adsorption of PEG is suppressed at these potentials too. Taking into account that the (100) face is much closer to the polycrystalline copper surface than the (111) face, and that the investigation of the adsorption of these species onto the (111) face is complicated by the simultaneous evolution of hydrogen, it seems reasonable to assume the above mentioned mechanism for the adsorption of SO_4^{2-}, Cl^- and PEG on polycrystalline copper surface. Hence, the adsorption of PEG as a neutral molecule has not been detected at potentials more negative than – 0.5 V *vs.* SSE, *e.g.,* in the region of copper

deposition from a copper acid bath containing these species. A weak "specific adsorption" of PEG has been recorded only in the absence of chloride ions.

Electrodeposition of copper in the presence of PEG and NaCl

The polarization diagrams obtained at a sweep rate of 1 m V s^{-1}, presented in Fig. 1, clearly indicate that the concentration of chloride ions is responsible for the ihibition of copper deposition in the presence of PEG in an acid copper bath. As can be seen, in a certain range of Cl^- concentrations (from 10^{-5} M to 10^{-4} M), the polarization diagrams are characterized by the presence of hysteresis, which is a real response of the system and not the cosequence of the sweep rate, as shown in Fig. 2 for diagrams obtained after prolonged polarization at a constant potential.

In conventional models of leveling it is assumed that adsorption of inhibiting additives is limited by diffusion as a consequence of the very low concentration of additives (10^{-6} M to 10^{-3} M) employed. Two limiting possibilities exist for transport control to be achieved: either the additive is consumed by reduction and subsequent desorption, or the molecule is incorporated into the growing deposit.[34,35] It is also possible, particularly for systems containing multi-component additives, to have a combination of these two effects. As it has been shown in the literature,[35] hysteresis in the voltammetric behaviour is a consequence of the competition between these various processes. As was shown recently by Moffat *et al.*[36] for copper electrodeposition in the presence of PEG, MPSA (3-mercapto-1-propanesulphonate) and NaCl, hysteresis arises from the competition between the inhibition provided by the Cl-PEG/Cu^{2+}/Cu^+/Cu interface and the catalytic effects of Cl-MPSA/Cu^{2+}/Cu^+/Cu interaction, which lead to an irreversible change in the reaction dynamics. No hysterisis, *i.e.,* no irreversible changes in the surface chemistry (reaction dynamics), was detected for the combination of Cl-PEG, or Cl-MPSA alone. It is important to note that in this paper the concentrations of NaCl, PEG and MPSA were kept constant at 10^{-3} M, 88.2×10^{-6} M and 1×10^{-5} M, respectively. It was also shown that superconformal electrodeposition of copper in 500 nm deep trenches, ranging from 500 nm to 90 nm in width, can be accomplished only from an electrolyte containing all three components. It was concluded that the hysteresis was a direct result of an alteration in the surface chemistry rather than a physical effect, *e.g.,* a diffusional relaxation associated with the scan direction, and that the hysteretic response reflects the competition between the rate of metal deposition and the accumulation and consumption of inhibiting additives.

Our results are in accordance with the results of Moffat *et al.*[36] to a certain point. As can be seen from Fig. 1, no hysteresis can be detected in the presence of 10^{-3} M NaCl, as was the case for Cl-PEG combination given in the paper of Moffat *et al.* (Ref. 36, Fig. 5). The appearance of hysteresis is most probably a direct result of an alteration of the surface chemistry rather than a physical effect and the hysteretic response might reflect the competition between the rate of metal deposition and the accumulation and consumption of inhibiting additives, but it is obvious from our results that hysteresis is not a consequence of competition between the inhibition provided by the Cl-PEG/Cu^{2+}/Cu^+/Cu interface and the catalytic effects of Cl-MPSA/Cu^{2+}/Cu^+/Cu interaction

as stated in the paper of Moffat *et al.,*[36] because hysteresis is also present in the solution containing only PEG and NaCl (Figs. 1 and 2). The results presented in Fig. 3 for different substrates also indicate that hysteresis could be a direct result of an alteration in the surface chemistry. It is obvious from these results that the inhibition of copper electrodeposition cannot be the consequence of chloride adsorption, since the same effects were obtained on three different substrates, one of them being glassy carbon on which chloride ions do not absorb.

The EIS measurements presented in Fig. 4 clearly indicate the simultaneuos occurrence of two processes in all the investigate solutions. One process is the discharge of Cu^{2+} ions and the deposition of copper presented in the equivalent circuit (Fig. 5) by the Faradaic resistance R_F and double layer capacitance C_{dl}. Another proecess is the specific adsorption and discharge of species containing molecules of the additive (PEG), presented in the equivalent circuit (Fig. 5) by the pseudo-capacitance C_p and the corresponding charge transfer resistance R_p. The second semi-circle, representing the presence of C_p and R_p, becomes well defined at concentrations of NaCl higher than 10^{-5} M, indicating a significant increase of C_p in comparison with C_{dl}. As can be seen in Fig. 6a, the double layer capacitance increases linearly with increasing current density of copper electrodeposition, most probably reflecting the increase in surface area (roughness) of the deposit. This increase is very small in the solution containing 10^{-3} M NaCl, with the double layer capacitance changig from about 12 μF cm^{-2} to about 20 μF cm^{-2}, which is reasonable to expect since the best leveling (superconformal deposition) effects are obtained with this concentration of NaCl.[36] The rate of copper deposition (R_F) is independent of NaCl concentration (Fig. 6b), while the rate of the discharge of specifically adsorbed species becomes faster at higher (10^{-4} M and 10^{-3} M) NaCl concentrations, *i.e.,* the values of R_p slightly decrease at these NaCl concentrations.

The most interesting and most intriguing feature of the EIS measurements is the exceptionally high value of the pseudo-capacitance recorded in the solutions containing 10^{-4} M and 10^{-3} M NaCl, as shown in Fig. 7. These values could be due either to the specific adsorption of heavily charged species, or to the increase in surface roughness. If they would be due to an increase in surface roughness, then the double layer capacitance should be influenced accordingly. Cosidering Fig. 6a, it is obvious that this is not the case and that the extremely high values of C_p are the consequence of specific adsorption of heavily charged species, or the competitive adsorption of several different species containing most probably Cu, PEG and Cl. It is interesting to note that the exceptionally high values of C_p are not in correlation with the appearance of hysteresis, indicating that the discharge of specifically adsorbed species is not responsible for the hysteretic response of the system.

Considering all the proposed mechanisms, it seems that none of them is sufficient for an explanation of the process of copper electrodeposition from an acid copper bath in the presence of PEG and NaCl.

In the model of Healy *et al.,*[17] it was assumed that a simple neutral PEG molecule is adsorbed at more negative potentials of copper electrodeposition. According to the differential capacitance measurements presented in Fig. 8, it is obvious that this is not

the case. Yokoi *et al.*[18,19] claim that positively charged complexes of the type $\{Cu^{+}(EO)_6\}$ become attracted by the negtively charged chloride ions specifically adsorbed onto the copper surface. This is also not possible since it is shown in pure chloride solution that the adsorbed chloride layer is completely discharged and that during UPD of cadmium this layer becomes replaced by cadmium atoms, with the chloride atoms remaining discharged on top of the cadmium layer.[37,38] Kelly *et al.*[23,24] developed a model that assumes adsorption of nearly a monolayer of PEG in the presence of chloride ions. This is also not in agreement with the differential capacitance measurements presented for the (100) face of copper in Fig. 8. Stoychev *et al.*[20] stated that in addition to the presence in the solution of simple chloride complexes of copper, such as $CuCl^{+}$, $CuCl_2$, $CuCl_3^{-}$ and $CuCl_4^{2-}$, complexes of the types $H^{+}\{–EO–\}_nCl^{-}$, $H^{+}\{–EO–\}_nCuCl_3^{-}$ and $H^{+}\{–EO–\}_nCuCl_2^{-}$ can also exist in the solution. Hence, it seems that it is practically impossible to predict a correct mechanism for copper electrodeposition in the presence of PEG and NaCl because of the presence of so many species, each of which could be able to contribute in the reaction of copper electrodeposition. The investigations presented in this paper clarified the adsorption behaviour of PEG and chloride ions and confirmed that some of the predicted models, assuming adsorption of neutral PEG molecule,[17,23,24] are not correct. It is obvious that a better understanding of the complex chemistry of the system is needed in order to determine the contribution of the species present in the solution to the process of copper electrodeposition.

CONCLUSIONS

Differential capacitance *vs*. potential curves recorded onto Cu(100) in solutions containing 0.1 M H_2SO_4, 0.1 M H_2SO_4 + 10^{-3} M PEG and 0.1 M H_2SO_4 + 10^{-3} M PEG + 10^{-3} M NaCl confirmed that "specific adsorption" of PEG molecules takes place in the absence of NaCl in the solution in the potential region of copper electrodeposition, *i.e.,* between – 1.0 V and – 0.5 V *vs*. SSE. In the presence of chloride ions the adsorption of PEG molecules is suppressed and there is no evidence for the adsorption of neutral PEG molecules. Accordingly, all models assuming the adsorption of neutral PEG molecules during copper electrodeposition cannot be correct.

It was shown that hysteresis, appearing on the polarization curves of copper electrodeposition, is not a consequence of competition between inhibition provided by the Cl-PEG/Cu^{2+}/Cu^{+}/Cu interface and the catalytic effects of Cl-MPSA/Cu^{2+}/Cu^{+}/Cu interaction, because hysteresis was also present in solutions containing only PEG and NaCl, *i.e.,* in the absence of MPSA.

EIS measurements confirmed the simultaneous occurrence of two processes during copper electrodeposition: the deposition of copper by the discharge of Cu^{2+} ions and "specific adsorption" and discharge of some heavily charged species, most probably containing Cu, PEG nad Cl.

И З В О Д

ЕЛЕКТРОХЕМИЈСКО ТАЛОЖЕЊЕ БАКРА ИЗ КИСЕЛОГ КУПАТИЛА У ПРИСУСТВУ ПОЛИЕТИЛЕН ГЛИКОЛА И ХЛОРИДА

В. Д. ЈОВИЋ и Б. М. ЈОВИЋ

Дрексел Универзитет, Филаделфија, ПА 19104, САД

Електрохемијско таложење бакра из киселог бакарног купатила (0,25 M $CuSO_4$ + 1,8 M H_2SO_4) у присуству полиетилен гликола (PEG) и натријум хлорида у веома малим концентрацијама (до 10^{-3} M), испитивано је мерењем поларизационих кривих, као и импедансним мерењима на Cu(111), Cu(100) и поликристалној бакарној електроди. Адсорпција сулфатних и хлоридних анјона, као и адсорпција PEG на Cu(111) и Cu(100) испитивана је цикличном волтаметријом и мерењем диференцијалног капацитета. Показано је да се PEG "специфично адсорбује" (уз размену наелектрисања) у раствору сулфата, док се у присуству хлоридних анјона адсорпција PEG не одиграва. Такође је показано да не долази до адсорпције неутралних молекула PEG на Cu(100), као и на поликристалу бакра. Установљено је да је инхибиција таложења бакра последица присуства хлоридних анјона. Појава "хистерезиса" на поларизационој кривој је такође у директној вези са концентрацијом хлорида у раствору. Резултати импедансних мерења су показали да се и у одсуству и у присуству хлорида при таложењу бакра одвијају две паралелне реакције: таложење бакра разелектрисањем Cu^{2+} јона и адсорпција и разелектрисање честица које у себи највероватније садрже Cu, PEG и Cl. При концентрацијама хлорида од 10^{-4} M и 10^{-3} M вредности "псеудо-капацитета" добијене фитовањем експерименталних резултата од око 0,02 F cm^{-2} до око 0,11 F cm^{-2} указују на чињеницу да адсорбоване честице поседују значајно наелектрисање, или да је у питању адсорпција и разелектрисање већег броја честица истовремено.

(Примљено 7. јуна 2001)

REFERENCES

1. J.W. H. Gauvin, C. A. Winkler, *J. Electrochem. Soc.* **99** (1952) 71
2. N. Pradhan, P. G. Krishna, S. C. Das, *Plating and Surface Finishing,* March (1996) 56
3. J. Crousier, I. Bimaghra, *Electrochim. Acta* **34** (1989) 1205
4. W. Plieth, *Electrochim. Acta* **37** (1992) 2115
5. D. Stoychev, I. Vitanova, R. Buyukliev, N. Petkova, I. Popova, I. Pojarliev, *J. Appl. Electrochem.* **22** (1992) 987
6. M. Wonsche, W. Dahms, H. Meyer, R. Schumacher, *Electrochim. Acta* **39** (1994) 1133
7. L. Fairman, *Metal Finishing,* July (1970) 45
8. D. Anderson, R. Haak, C. Ogden, D. Tench, J. White*, J. Appl. Electrochem.* **15** (1985) 631
9. L. Mayer, S. Barbieri, *Plating and Surface Finishing,* March (1981) 46
10. E. Mattson, J. O'M. Bockris, *Trans. Faraday Soc.* **55** (1959) 1586
11. J. O'M. Bockris, J. Kita, *J. Electrochim. Soc.* **109** (1962) 928
12. O. R. Brown, H. R. Thirsk, *Electrochim. Acta* **10** (1965) 383
13. J. O'M. Bockris, G. Razumney, *J. Electroanal. Chem.* **41** (1973) 1
14. J. O'M. Bockris, M. Enyo, *Trans. Farady Soc.* **58** (1962) 1187
15. E. Chassaing, R. Wiart, *Electrochim. Acta* **29** (1984) 649
16. M. R. H. Hill, C. T. Rogers, *J. Electroanal. Chem.* **86** (1978) 179
17. J. P. Healy, D. Pletcher, *J. Electroanal. Chem.* **338** (1992) 155
18. M. Yokoi, S. Konishi, T. Hayashi, *Denki Kagaku* **52** (1984) 218

19. M. Yokoi, S. Konishi, T. Hayashi, *Denki Kagaku* **51** (1983) 460
20. D. Stoychev, C. Tsvetanov, *J. Appl. Electrochem.* **26** (1996) 741
21. D. Stoychev, I. Vitanova, T. Vitanov, S. Rashkov, *Surf. Technol.* **7** (1978) 427
22. D. Stoychev, I. Vitanova, T. Vitanov, S. Rashkov, *C. R. Bulg. Acad. Sci.* **32** (1979) 1515
23. J. J. Kelly, A. C. West, *J. Electrochem. Soc.* **145** (1998) 3472
24. J. J. Kelly, A. C. West, *J. Electrochem. Soc.* **145** (1998) 3477
25. V. D. Jović, B. M. Jović, R. Parsons, *J. Electroanal. Chem.* **290** (1990) 257
26. V. D. Jović, R. Parsons, B. M. Jović, *J. Electroanal. Chem.* **339** (1992) 327
27. B. M. Jović, V. D. Jović, D. M. Dražić, *J. Electroanal. Chem.* **399** (1995) 197
28. A. N. Frumkin, B. B. Damaskin, in *Modern Aspects of Electrochemistry*, J. O'M. Bockris, Ed., Vol. 3, Academic Press Inc., New York, 1964
29. M. Wilms, P. Broekmann, M. Kruft, Z. Park, C. Schtulmann, K. Wendelt, *Surf. Sci.* **402** (1998) 83
30. M. Wilms, P. Broekmann, C. Schtulmann, K. Wendelt, *Surf. Sci.* **416** (1998) 121
31. E. Gileadi, *Electrode Kinetics for Chemists, Chemical Engineers and Materials Scientists,* VCH, New York, 1993
32. D. Suryanarayana, P. A. Narayana, L. Kevan, *Inorg. Chem.* **22** (1983) 474
33. C. B. Ehlers, I. Villegas, J. L. Stickney, *J. Electroanal. Chem.* **284** (1990) 403
34. C. Madore, M. Matlosz, D. Landolt, *J. Electrochem. Soc.* **143** (1996) 3927
35. D. Roha, U. Landau, *J. Electrochem. Soc.* **137** (1990) 824
36. T. P. Moffat, J. E. Bonevich, W. H. Huber, A. Stanishevsky, D. R. Kelly, G. R. Stafford, D. Josell, *J. Electrochem. Soc.* **147** (2000) 4524
37. C. Schtulmann, Z. Park, C. Bach, K. Wendelt, *Electrochim. Acta* **44** (1998) 993
38. V. D. Jović, B. M. Jović, *J. Serb. Chem. Soc.,* **66** (2001) 345.